



Nuclear mitochondria-related genes-based molecular classification and prognostic signature reveal immune landscape, somatic mutation, and prognosis for glioma

Chang Liu^{a,b,c,1}, Ning Zhang^{b,d,e,1}, Zhihao Xu^{b,d,f,1}, Xiaofeng Wang^b, Yang Yang^{b,d}, Junming Bu^{b,c}, Huake Cao^{b,d}, Jin Xiao^{f,**}, Yinyin Xie^{a,*}

^a College of Life Sciences, Anhui Medical University, Hefei, 230032, Anhui, China

^b School of Basic Medical Sciences, Anhui Medical University, Hefei, 230032, Anhui, China

^c Second School of Clinical Medicine, Anhui Medical University, Hefei, 230032, Anhui, China

^d First School of Clinical Medicine, Anhui Medical University, Hefei, 230032, Anhui, China

^e Department of Obstetrics and Gynecology, The First Affiliated Hospital of Anhui Medical University, Hefei, 230022, Anhui, China

^f Department of Neurosurgery, First Affiliated Hospital of Anhui Medical University, Hefei, 230022, Anhui, China

ARTICLE INFO

Keywords:

Prognosis

Nuclear mitochondria-related genes

Glioma

Machine learning

Tumor microenvironment

MGME1

ABSTRACT

Background: Glioma is the most frequent malignant primary brain tumor, and mitochondria may influence the progression of glioma. The aim of this study was to analyze the role of nuclear mitochondria related genes (MTRGs) in glioma, identify subtypes and construct a prognostic model based on nuclear MTRGs and machine learning algorithms.

Methods: Samples containing both gene expression profiles and clinical information were retrieved from the TCGA database, CGGA database, and GEO database. We selected 16 nuclear MTRGs and identified two clusters of glioma. Prognostic features, microenvironment, mutation landscape, and drug sensitivity were compared between the clusters. A prognostic model based on multiple machine learning algorithms was then constructed and validated by multiple datasets.

Results: We observed significant discrepancies between the two clusters. Cluster One had higher nuclear MTRG expression, a lower survival rate, and higher immune infiltration than Cluster Two. For the two clusters, we found distinct predictive drug sensitivities and responses to immune therapy, and the infiltration of immune cells was significantly different. Among the 22 combinations of machine learning algorithms we tested, LASSO was the most effective in constructing the prognostic model. The model's accuracy was further verified in three independent glioma datasets. We identified *MGME1* as a vital gene associated with infiltrating immune cells in multiple types of tumors.

Conclusion: In short, our research identified two clusters of glioma and developed a dependable prognostic model based on machine learning methods. *MGME1* was identified as a potential biomarker for multiple tumors. Our results will contribute to precise medicine and glioma management.

* Corresponding author.

** Corresponding author.

E-mail addresses: xjtulip@163.com (J. Xiao), xieyinyin@ahmu.edu.cn (Y. Xie).

¹ Chang Liu, Ning Zhang, and Zhihao Xu contributed equally to this work.

1. Introduction

Glioma is a prevalent form of tumor that accounts for a significant proportion of primary malignant brain tumors in adults, comprising 80% of such cases [1]. Despite representing only 2% of all primary cancers, gliomas have been found to lead to 7% of deaths among individuals under the age of 70 [2]. Because it behaves aggressively and almost cannot be cured by current treatments, glioma is regarded as one of the most destructive and traumatic cancers [3]. It has a 5-year survival of 35% with many clinical symptoms, seriously affecting patients' quality of life [4]. Approximately 50–80% of patients with glioma develop seizures, while 15% patients have symptom of increased intracranial pressure, resulting in high symptomatic burden [5,6]. Despite advancements in cancer therapies, few methods have been applied in glioma due to cancer heterogeneity and the blood brain barrier [7]. The effective management of glioma is still a great challenge.

According to the WHO 2021 classification of gliomas, gliomas should be subdivided not only by histological diversity but also by molecular data. This trend is reflective of the growing understanding that the identification of specific molecular alterations, such as those involving MYB, MN1, and BCOR, plays a significant role in determining the type of glioma [8,9]. In the past decade, scientists have found many biomarkers for glioma, including mutations in special families and common inherited variants in independent genetic loci [10]. Recently, the advent of comprehensive molecular analysis techniques and bioinformatics has had a large impact on tumor research and treatment [10]. Many studies have explored the molecular biomarkers of glioma to enable accurate disease prediction with the goal of improving the treatment and prognosis of glioma. Some molecular biomarkers such as MEOX2 [11], PDIA5 [12], and DDX3X [13], possess strong predictive capabilities. However, the molecular mechanisms underlying glioma remain unclear due to its complexity.

Mitochondria perform many interconnected functions including energy metabolism and cell apoptosis, playing an important part in neoplastic development. Mitochondria can support cancer cell growth and survival in harsh environments [14,15]. Nuclear mitochondria-related genes (nuclear MTRGs) are the mitochondria-related genes encoded by the nuclear genome, whose protein products are imported into mitochondria following cytoplasmic synthesis [16,17]. These proteins from the nucleus play important roles in the mitochondria-related genes related processes, such as replication, transcription, degradation, and the occurrence and development of tumors. For example, MFN1 is able to promote tethering and fusion of the outer mitochondrial membrane and DRP1 promotes mitochondrial fission. Knockdown of MFN1 or forced overexpression of DRP1 can promote mitochondrial division, enhancing the viability of hepatocellular carcinoma cells [18–20]. Previous studies have shown that mitochondrial dysfunction has a strong connection to the development and treatment of glioma [21–23]. However, the function of the nuclear MTRGs in cancer has not been fully studied.

In the current study, we first identified differentially expressed nuclear MTRGs in glioma using open data including mRNA expression profiles and the corresponding clinical information of glioma patients. Subsequently we performed a clustering analysis on the TCGA cohort. We compared the abundance of various immune cells and the expression of immune checkpoint-related genes (ICRGs), and predicted the effect of immune checkpoint blockade (ICB) therapy and drug sensitivity between the clusters. We then developed a prognostic model for glioma utilizing multiple machine learning algorithms, which has been demonstrated to possess a high level of reliability. A single gene, *MGME1*, was selected for further examination. We investigated the expression and function of *MGME1* in glioma, and pan-cancer analysis was applied for further research in terms of expression and immune relevance. Our study provides novel insights into the molecular mechanism associated with the tumor-immune microenvironment and mutations in glioma and helps enhance patient stratification and personalized treatment of glioma.

2. Materials and methods

2.1. Data collection and processing

The RNA-sequencing expression profiles and clinical information of 666 glioma samples were collected from TCGA (<https://tcga-data.nci.nih.gov/tcga/>). Normal tissues were downloaded from Genotype-Tissue Expression (GTEx, <http://commonfund.nih.gov/GTEx/>). In addition, we collected 325 tumor samples from CGGA (<http://www.cgga.org.cn/>) and 180 tumor samples from GSE184941, GEO (<https://www.ncbi.nlm.nih.gov/gds/>) to verify our prognostic model. The nuclear MTRGs were obtained from MITOMAP (<http://www.mitomap.org/>). All nuclear MTRGs (including 114 nonstructural nuclear MTRGs and 33 structural nuclear MTRGs) were grouped into one gene set called “MTRGs” for subsequent analysis. The online tool Sangerbox was used to sort and organize the clinical information [24].

2.2. Recognition of differentially expressed genes in glioma

To identify the differentially expressed nuclear MTRGs, we used the “limma” package in R software to study the mRNA [25]. Glioma samples from the TCGA database and normal samples from the GTEx database were used. “Adjusted $P < 0.05$ and $|\text{Log}_2(\text{Fold Change})| > 1$ ” were set as the threshold for selection. Then we calculated the intersections between nuclear MTRGs and differentially expressed genes (DEGs) through Venn diagrams (<http://bioinformatics.psb.ugent.be/webtools/Venn/>).

The potential mechanism of the differentially expressed nuclear MTRGs were explored by Gene Ontology (GO) and Kyoto Encyclopedia of Genes and Genomes (KEGG) using the “ClusterProfiler” R package. The R packages “ggplot2” and “pheatmap” were used to draw the boxplot and heatmap [26]. P value < 0.05 and FDR < 0.1 were considered statistically significant.

2.3. Consensus cluster analysis for glioma based on nuclear MTRGs

A total of 16 genes were selected by the least absolute shrinkage and selection operator (LASSO) regression algorithm from the DEGs. This procedure was performed using the “glmnet” R package, and 10-fold cross-validation was used. Kaplan-Meier (KM) survival curves were generated by using GEPIA2 [27].

The selected 16 genes were then used to generate a consistency analysis with the “ConsensusClusterPlus” R package (v1.54.0) in the TCGA cohort, and the number of the clusters was set as two [28]. Eighty percent of the samples were taken at random, innerLinkage = “ward.D2”, clusterAlg = “hc”. For the KM curves, we used log-rank tests to compare the two groups. Under a 95% confidence interval, hazard ratio (HR) and *P* value were calculated by log-rank tests and univariate Cox proportional hazards regression. We used the “ggplot2” and “ggsci” R packages to perform principal component analysis (PCA).

2.4. Immune infiltration between two clusters

To obtain accurate immune scores, the “immunedeconv” R package was used [29]. TIMER was applied to compare the immune cell score between the two clusters. CIBERSORT was used to estimate the abundance percentage of immune cells infiltrating tumors in each tumor tissue. Different colors represent different kinds of immune cells. For immune checkpoints, we screened eight ICRGs, TIGIT, SIGLEC15, CD274, CTLA4, PDCD1, PDCD1LG2, LAG3, and HAVCR2, and compared their expression. This step was finished with the “ggplot2” R package and “heatmap” R package. We then used Tumor Immune Dysfunction and Exclusion (TIDE) to predict the ICB response. *P* < 0.05 was considered statistically significant.

2.5. Mutation landscape between two clusters

The mutation landscape showed the mutated genes and the frequency of variants using the “maftools” R package [30]. We compared the mutation rates by the “ggplot2” R package.

2.6. Drug sensitivity prediction

We predicted the efficacy of four common drugs used for the treatment of glioma with the “oncoPredict” R package and the training set from the GDSC dataset (<https://www.cancerrxgene.org/>) [31]. A lower IC50 value represents higher sensitivity, and the boxplot was generated using the “ggplot2” R package.

2.7. Construction and validation of a nuclear MTRG signature for glioma

The data from the TCGA database was divided into a training set and a validation set at a ratio of 7:3. The counts data with corresponding clinical data were transformed to TPM and changed to log₂(TPM+1) format. To construct a prognostic model, 22 combinations of ten machine learning algorithms, including RSF, GBSA, SSVM, SDL, Enet, Stepwise Cox, Coxboost, SuperPC, plsRcox, and LASSO, were used and trained based on the TCGA training set and the selected 16 genes. The full name of each algorithm is shown in [Supplementary Table 1](#). TCGA validation set, CGGA dataset, and GSE184941 were used to estimate the effect of different algorithms and screen out the most valuable nuclear MTRG signature with the highest Area Under Curve (AUC). The nuclear MTRG signature was established by the Python scikit-survival library (version 0.19.0) and the “randomForestSRC”, “glmnet”, “plsRcox”, “superpc”, and “CoxBoost” R packages [32,33]. The immunohistochemical figures were retrieved from the HPA database (<https://www.proteinatlas.org/>).

2.8. Selection and analysis of MGME1

Among the genes in the prognostic model, univariate and multiple Cox regression analysis were performed to select the single gene with the strongest prognostic ability. The Tumor Mutation Burden (TMB) score, microsatellite instability (MSI) score, and TIDE score were compared between the high-expression and low-expression groups of MGME1. The “TIMER” R package was applied to calculate the relationship between the expression of MGME1 and the abundance of infiltrating immune cells.

2.9. Pan-cancer analysis

The RNA-sequencing expression profiles and corresponding clinical data were downloaded from the TCGA database. The expression of MGME1 in 33 types of tumor tissues and the corresponding normal tissues was compared. The immune score of MGME1 in all types of tumors was shown using the “immunedeconv” R package. The relationship between the expression of immune-checkpoint-related genes and MGME1 in multiple types of tumors was visualized by the “heatmap” R package. A significance level of *P* < 0.05 indicated a significant difference.

3. Results

3.1. Identification of the differentially expressed nuclear MTRGs in glioma

We used TCGA and GTEx databases to select DEGs between glioma and normal tissues. The result of the “limma” R package analysis was shown in [Supplementary Table 2](#). A volcano plot displayed the overall gene expression in glioma and a total of 10,065 DEGs were identified ([Fig. 1A](#)). To determine the intersection between the nuclear MTRGs and DEGs, a Venn diagram was employed, and 97 genes

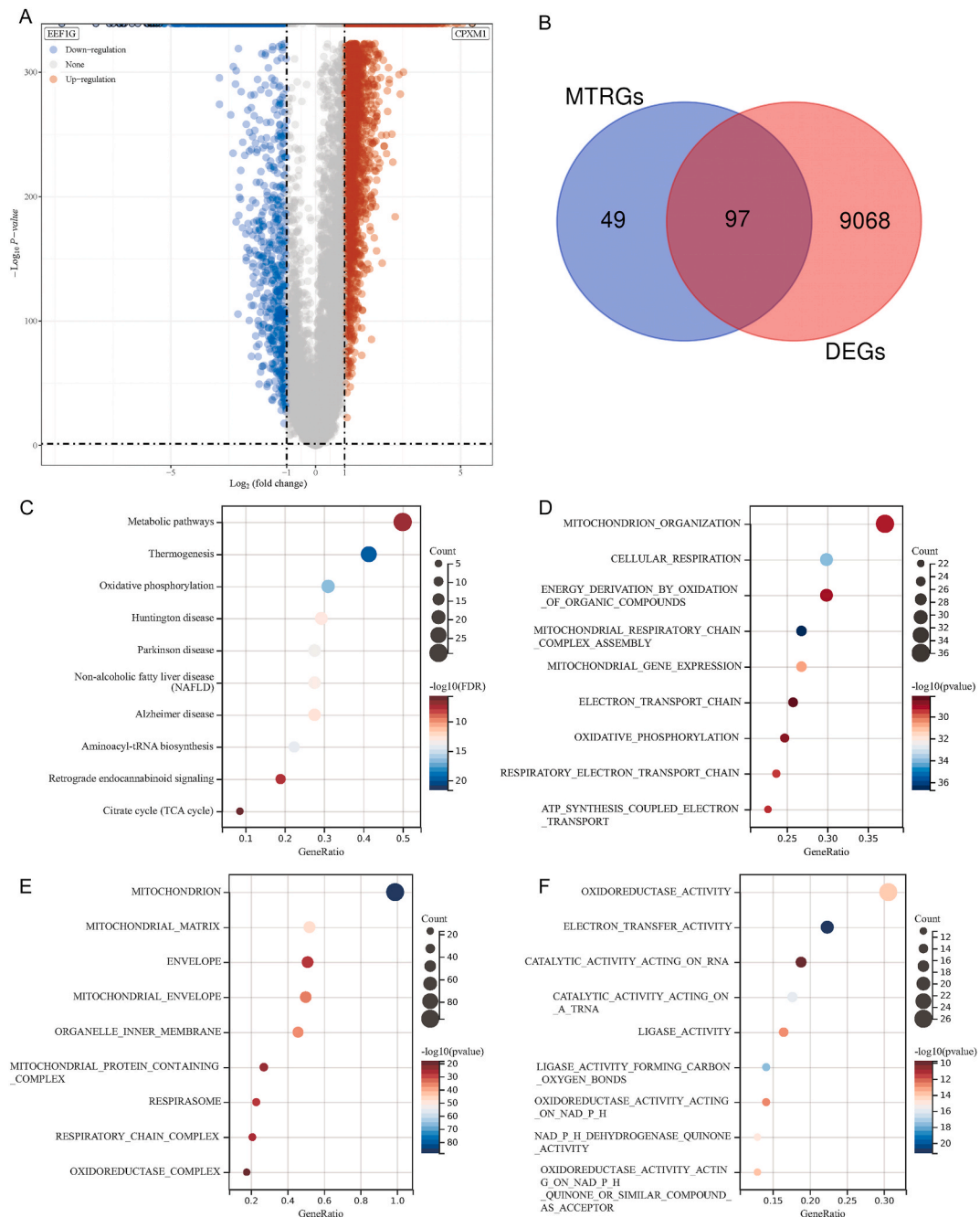


Fig. 1. Heatmap and Venn diagram of DEGs and nuclear MTRGs. (A) DEGs of the TCGA dataset. Red represents significantly upregulated genes; blue represents significantly downregulated genes. (B) Venn diagram of the differentially expressed nuclear MTRGs. (C–F) The enriched KEGG signaling pathways (C), GO cellular components analysis (D), GO biological processes analysis (E), and GO molecular functions analysis (F) of the 97 selected nuclear MTRGs. Different colors represent the corresponding significance of the P value.

were selected (Fig. 1B). To explore the function of the 97 selected genes, we performed KEGG pathway analysis and GO enrichment analysis for the selected genes. The KEGG results indicated that these genes were mainly involved in metabolic pathways and thermogenesis (Fig. 1C). In the GO analysis, we found that these genes were highly related to mitochondria, oxidoreductase activity, and electron transfer reaction (Fig. 1D–F).

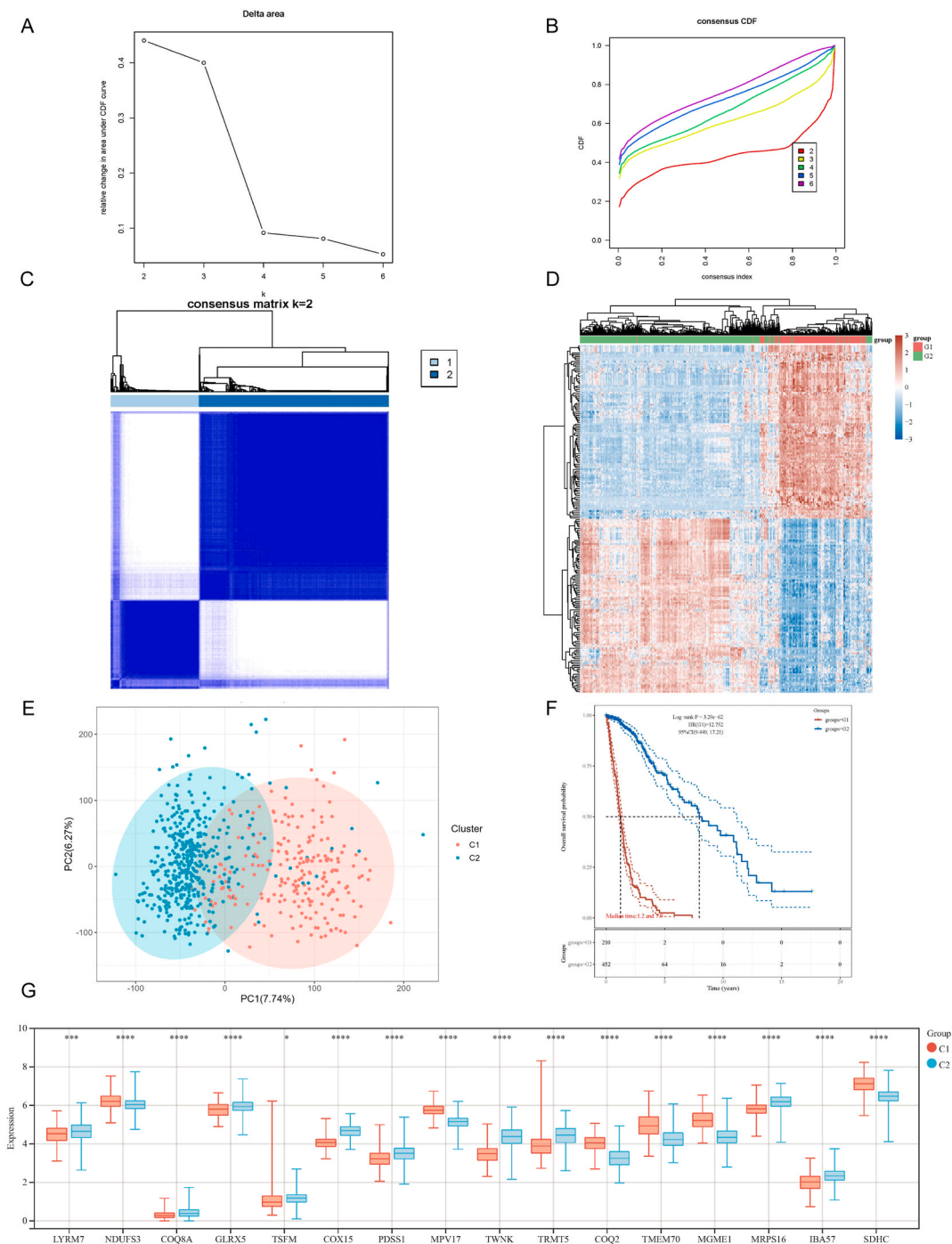


Fig. 2. Consensus clustering analysis of nuclear MTRGs. (A, B) CDF and relative change in the area under the CDF curve (CDF Delta area). (C) Heatmap for clustering. (D) Heatmap of gene expression in different clusters. Red represents high expression and blue represents low expression. (E) The PCA shows the difference between the two clusters. (F) The overall survival of the two clusters is shown by KM curves. (G) The expression of the 16 selected nuclear MTRGs was compared between Cluster One and Cluster Two. (* $P < 0.05$, ** $P < 0.01$, *** $P < 0.001$, and **** $P < 0.0001$).

3.2. Consensus clustering analysis of nuclear MTRGs revealed a significant distinction between two clusters

To select key genes for the prognosis of glioma, we used the LASSO algorithm and identified 16 genes of the 97 selected nuclear MTRGs (Supplementary Fig. 1A, 1B). The KM curves of the 16 selected nuclear MTRGs are presented in Supplementary Fig. 2A-P. All the genes were differentially expressed in glioma (Supplementary Fig. 2Q). We then conducted consensus clustering analysis using these 16 genes. Considering the ratio of ambiguous clustering metrics and the expression levels of the identified nuclear MTRGs, we determined that $k = 2$ is the optimal clustering stability among the range of k values from 2 to 6 (Fig. 2A, 2B). According to these criteria, the patients from TCGA were divided into two groups: Cluster One with 213 samples and Cluster Two with 453 samples (Fig. 2C). The two clusters displayed opposite gene expression patterns and were clearly separated (Fig. 2D, E). However, the two clusters did not show any statistically significant differences in terms of gender or racial distribution (Table 1). The patients in Cluster Two had a longer survival rate (median OS: 1.3 years for Cluster One and 7.9 years for Cluster Two, Fig. 2F). All 16 nuclear MTRGs were significantly differentially expressed between the two clusters (Fig. 2G).

3.3. Immune microenvironment and ICB therapy efficacy between the two clusters

As illustrated in Fig. 3A, Cluster One exhibited a higher level of immune cell infiltration, including CD8⁺ T cells, neutrophils, myeloid dendritic cells, and macrophages than Cluster Two. The percentage of immune cells was visualized through heatmap (Fig. 3B). The expression of eight ICRGs was also compared between the clusters. Except for *TIGIT*, all these genes including *CD274* had an increased expression level in Cluster One (Fig. 3C). We further evaluated the different effects of immune checkpoint blockade (ICB) therapy on patients from the two clusters using TIDE scores. The results indicated a higher score in Cluster One than Cluster Two, which meant that patients in Cluster One had higher response rate to ICB therapy (Fig. 3D). Previous studies have proven that TMB is related to the therapeutic efficacy of ICB for glioma patients, and MSI-high tumors have a promising response to ICB [34,35]. We compared the TMB score (Fig. 3E) and MSI score (Fig. 3F) between the two clusters. However, the results indicated that Cluster One had a higher TMB and lower MSI (Fig. 3E, F).

3.4. The nuclear MTRGs based cluster was associated with drug sensitivity

The drug sensitivity of four commonly utilized chemotherapy agents for glioma [36,37] was investigated between the two clusters. The results suggested that Temozolomide (Fig. 3G), Carmustine (Fig. 3H), and Dabrafenib (Fig. 3J) displayed improved efficacy in Cluster Two. Trametinib had better efficacy in Cluster One (Fig. 3I).

3.5. Mutation landscapes and drug sensitivity of the two glioma clusters

As shown in Fig. 4A, we drew the mutation landscapes of glioma and highlighted the top ten genes exhibiting the highest mutation frequency. Patients in Cluster Two had a higher mutation frequency than patients in Cluster One (Fig. 4B, C). The predominant mutation observed in both clusters was missense mutation with single nucleotide polymorphism being more frequent than insertion and deletion (Fig. 4B, C). We then chose four key genes that displayed important roles in the development of glioma as previously reported [38,39]. The comparison of samples carrying mutations between the two clusters was conducted for these four genes (Fig. 4D, E, Supplementary Fig. 3). Patients in Cluster Two had a higher IDH1 mutation rate, a lower EGFR mutation rate, and a higher IDH2 mutation rate than patients in Cluster One (Fig. 4D-F), whereas the mutation of *TERT* appeared to be uncorrelated with the clusters (Supplementary Fig. 3).

Table 1
Clinical characteristics between the two clusters.

Characteristics	C1	C2	P value
n	213	453	
Vital status demographic, n (%)			<0.001
Alive	47 (7.1%)	365 (54.8%)	
Dead	164 (24.6%)	87 (13.1%)	
Not Reported	2 (0.3%)	1 (0.2%)	
Gender demographic, n (%)			0.077
female	80 (12%)	203 (30.5%)	
male	133 (20%)	250 (37.5%)	
Age at initial pathologic diagnosis, median (IQR)	59 (52, 67)	39 (31, 49)	<0.001
Race demographic, n (%)			0.019
white	189 (28.4%)	421 (63.2%)	
not reported	1 (0.2%)	10 (1.5%)	
asian	6 (0.9%)	7 (1.1%)	
black or African american	16 (2.4%)	15 (2.3%)	
American Indian or alaska native	1 (0.2%)	0 (0%)	
Radiation therapy, n (%)			<0.001
YES	161 (27.3%)	239 (40.6%)	
NO	30 (5.1%)	159 (27%)	

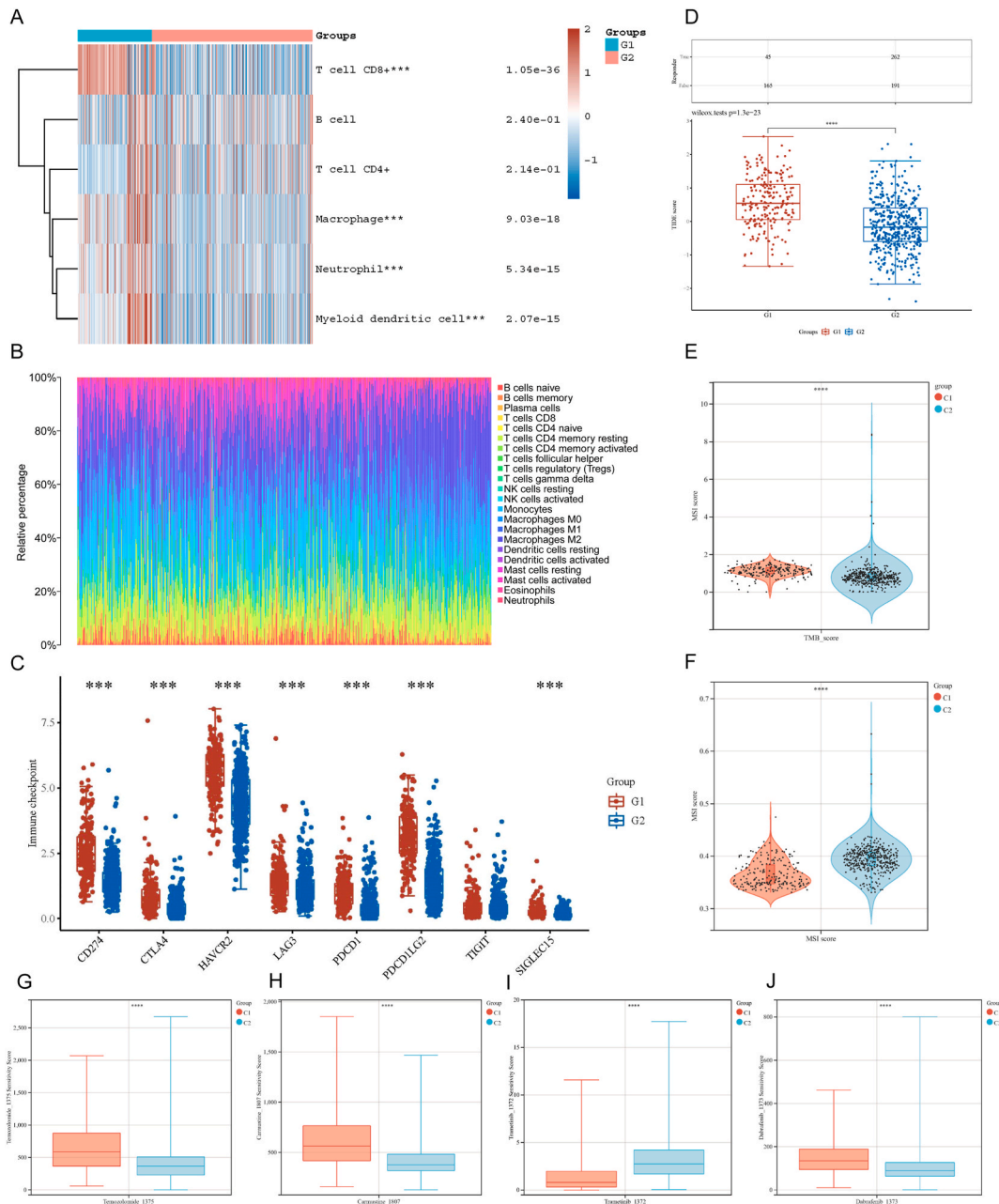


Fig. 3. Tumor microenvironment in the two clusters. (A–B) Infiltration level of several immune cells in the two glioma clusters (A) and the percentage of immune cells in tumor tissues (B). Different colors represent the corresponding immune cells. (C–F) The expression of the ICRGs (C), TIDE score (D), TMB score (E), and MSI score (F) of the two clusters. (G–J) Predicted sensitivity scores of Temozolomide (G), Carmustine (H), Trametinib (I), and Dabrafenib (J). (*P < 0.05, **P < 0.01, ***P < 0.001, and ****P < 0.0001).

3.6. Development of a prognostic signature for glioma using machine learning algorithms

To construct MTRG prognostic signatures for glioma, we performed ten machine learning algorithms including RSF, GBSA, SSVM, SDL, Enet, Stepwise Cox, Coxboost, SuperPC, plsRcox, and LASSO based on the previously selected 16 nuclear MTRGs. A total of 22 combinations were generated and 10-fold cross-validation was applied to find the most effective and reliable signature with the highest AUCs in the three validation sets (TCGA validation set, CGGA, and GSE184941) (Fig. 5A). The results indicated that LASSO had the highest AUC with an average value of 0.868, and was identified as the most effective model. To further verify the model, we utilized the LASSO model to divide each of the above four datasets into a high-score group and a low-score group. The high-score group had a relatively lower survival rate, indicating the reliability of our prognostic model (Fig. 5B-D).

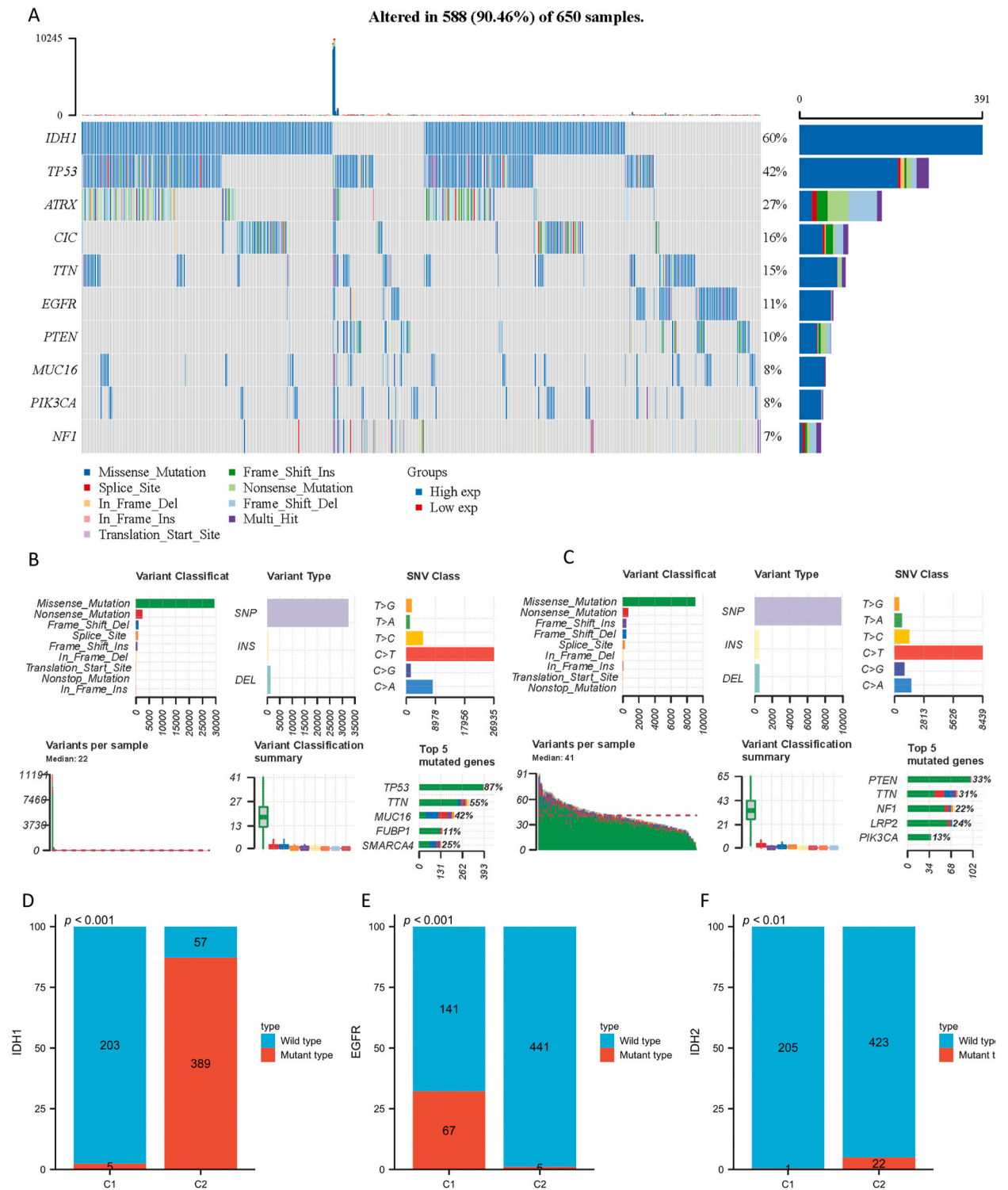


Fig. 4. Mutation landscape of the two clusters. (A) Oncoplot shows the somatic landscape of the glioma cohort. (B, C) The cohort summary plots for Cluster One (B) and Cluster Two (C) show the distribution of variants. (D–F) We compared the mutation of IDH1 (D), EGFR (E), and IDH2 (F) between the two clusters.

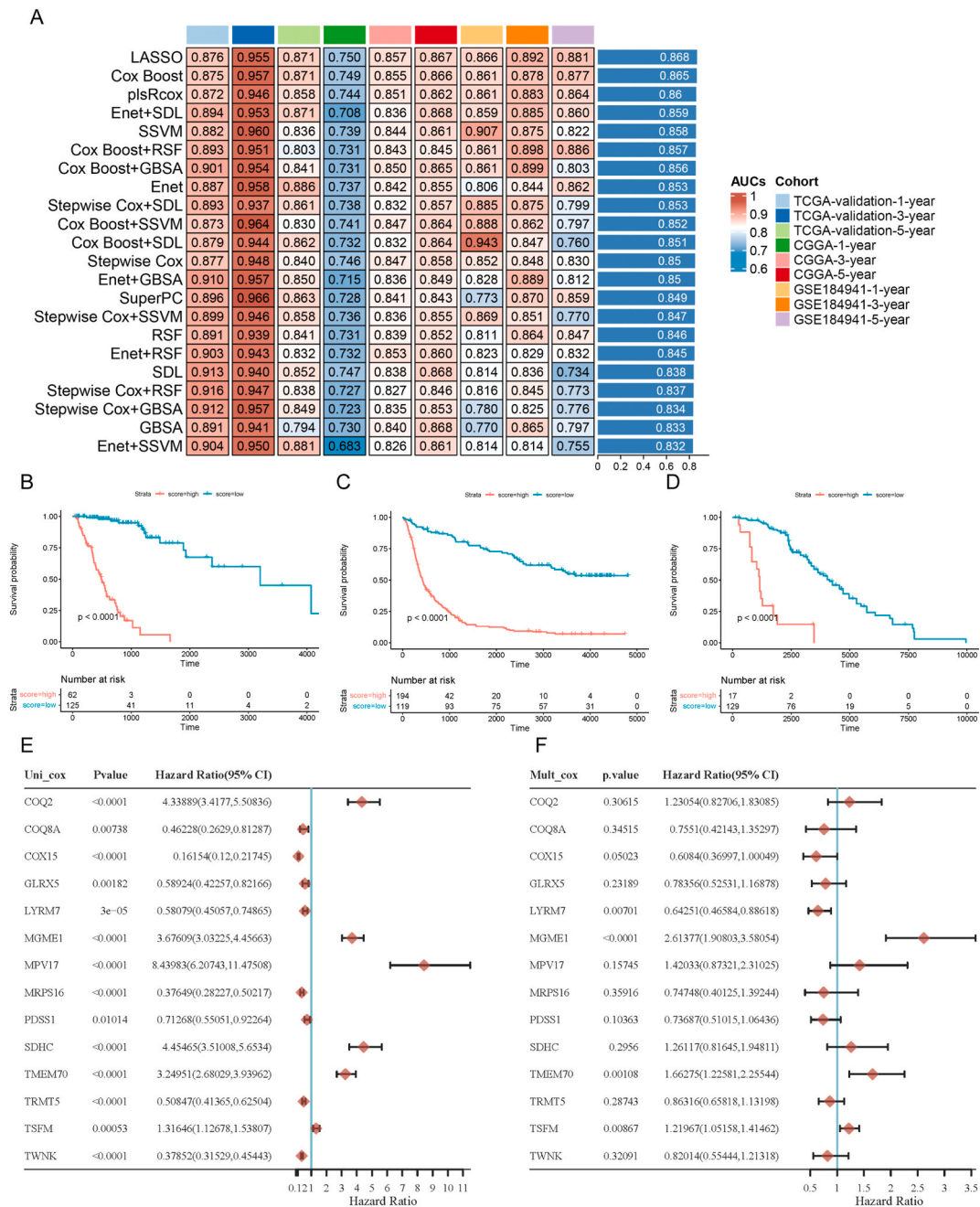


Fig. 5. The prognostic value of the nuclear MTRG signatures. (A) A total of 22 combinations of machine learning algorithms for the nuclear MTRG signatures. The AUCs of each model at 1, 3, and 5 years were calculated based on different datasets, including the TCGA validation set, CGGA, and GSE184941. (B–D) The KM curves of the high-risk and low-risk patients in the TCGA validation set (B), CGGA (C), and GSE184941 (D). Univariate and multiple Cox regression analysis were performed on the 9 genes in the signature (E–F).

3.7. Identification of *MGME1* as a key gene for glioma

Based on the selected 16 nuclear MTRGs, univariate and Cox regression analysis were utilized to select the genes with strong prognostic ability. *MGME1* was identified for its strong prognostic ability (Fig. 5E and F), indicating its crucial role in the progression of glioma. High expression of *MGME1* was associated with a lower survival rate (Fig. 6A). The immunohistochemical results from the HPA database indicated the high expression of *MGME1* in glioma tissue (Fig. 6E). In addition, TMB score (Fig. 6B), MSI score (Fig. 6C), and TIDE score (Fig. 6D) between the high-expression and low-expression groups exhibited significant differences.

The expression of *MGME1* was also associated with the tumor microenvironment (Fig. 6F–K). *MGME1* expression was found to be

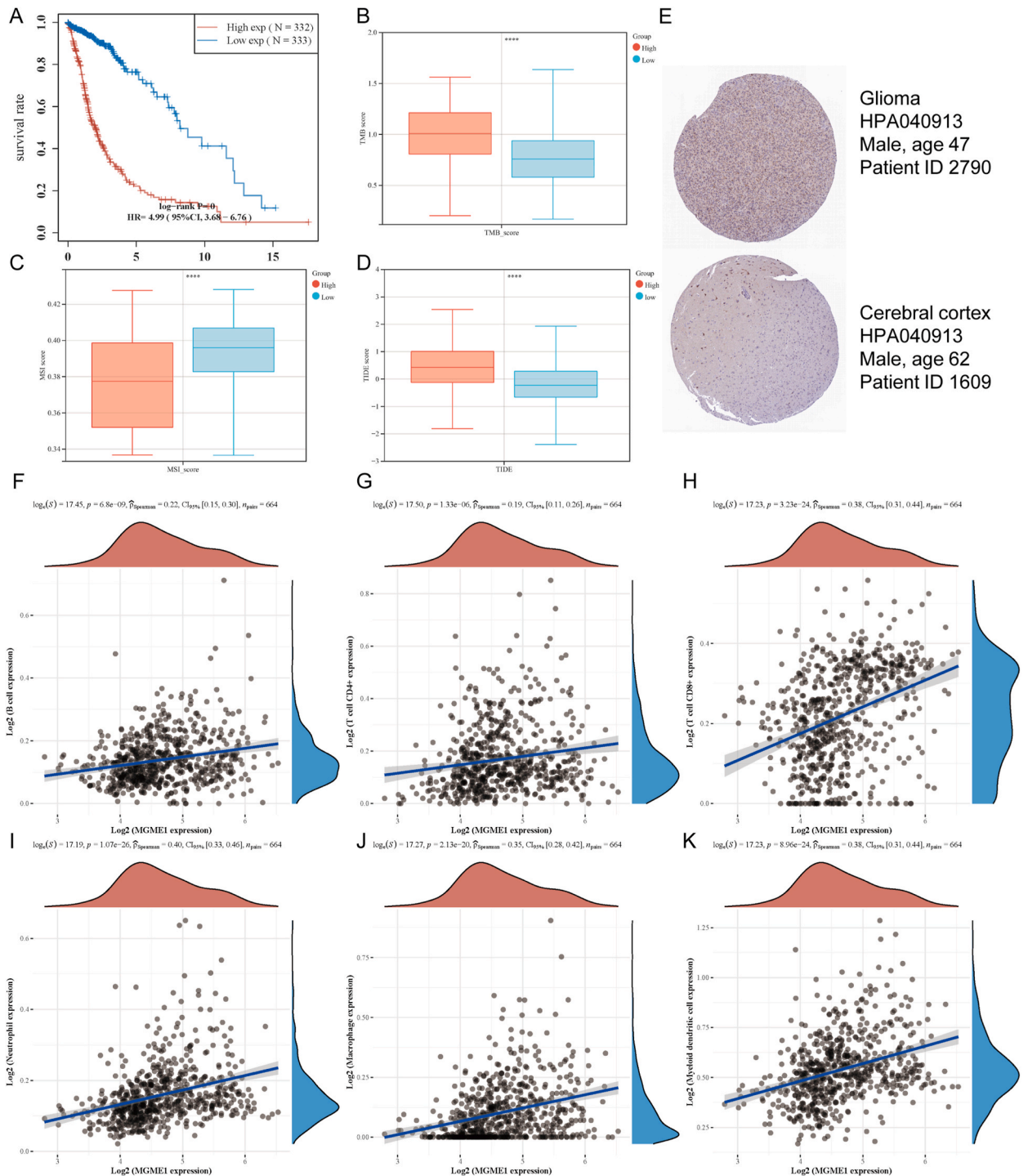


Fig. 6. The function of *MGME1* in glioma. (A) KM curves of the high and low *MGME1* expression groups. TMB score (B), MSI score (C), and TIDE score (D) in the high and low *MGME1* expression groups. (E) The immunohistochemical results of *MGME1* from the HPA database. (F–K) The relationship between the expression of *MGME1* and the abundance of immune cells.

significantly correlated with the abundance of B cells, CD4⁺ T cells, CD8⁺ T cells, neutrophils, macrophages, and endothelial cells.

3.8. Pan-cancer analysis of *MGME1* across human tumors

Considering the key role of *MGME1* in glioma, we further explored the function of *MGME1* across 33 human tumors. The full names of the tumors are presented in [Supplementary Table 3](#). First, the relative expression of *MGME1* was analyzed using the GTEx and TCGA databases ([Fig. 7A-D](#)). The results indicated that *MGME1* was significantly upregulated in 27 tumor types (ACC, BLCA, BRCA, CESC, CHOL, COAD, DLBC, ESCA, GBM, HNSCT, KIRC, KIPR, LGG, LIHC, LUAD, LUSC, OV, PAAD, PRAD, READ, SARC, SKCM, STAD, TGCT, THCA, UCEC, and USC, $P < 0.001$), and downregulated in PCPG ($P < 0.001$). Furthermore, *MGME1* was closely related to the tumor microenvironment in multiple kinds of tumors, including KICH, KIRC, LGG, LIHC, LUSC, MESO, OV, PAAD, PCPG, PRAD, READ, SKCM, THCA and THYM ([Fig. 7E](#)). In addition, *MGME1* had a strong relationship with the expression of the ICRGs in COAD, KICH, KIRC, LIHC, LUSC, MESO, PAAD, PRAD, SKCM, THCA, THYM, UCEC, and UVM ([Fig. 7F](#)). The expression of *MGME1* was also correlated with TMB and MSI in multiple tumors ([Supplementary Fig. 4A,4B](#)). In short, *MGME1* may function as a molecular biomarker across human tumors.

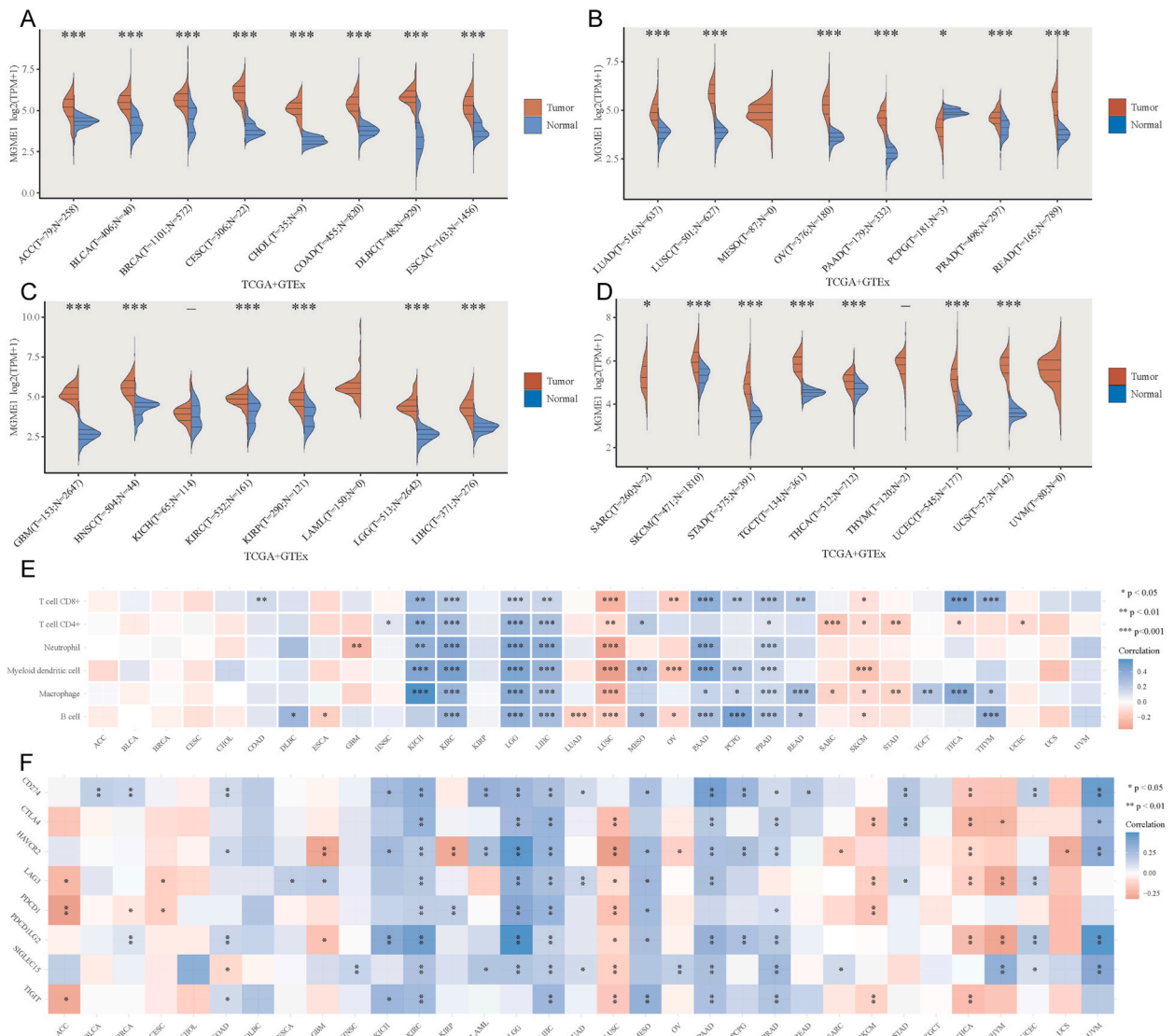


Fig. 7. Pan-cancer analysis of *MGME1*. (A–D) *MGME1* is differentially expressed in 27 tumor types. *MGME1* expression is related to the abundance of cells in the tumor microenvironment (E) and the expression of ICRGs (F) in a variety of tumor types. (* $P < 0.05$, ** $P < 0.01$, *** $P < 0.001$).

4. Discussion

Gliomas are the most common tumors within the central nervous system and are characterized by their high proliferation and invasiveness potential [40]. Despite the use of debulking surgery, chemotherapy, and adjuvant radiotherapy, the survival prospects of individuals remain constricted, with a median survival rate of 12–15 months [41]. The management of glioma still requires improvement, and effective prognostic models are desperately needed.

Reactive oxygen species (ROS) are byproducts of the formation of ATP. A low level of ROS functions as an antitumor agent, whereas an abnormal level of ROS was reported to be related to the development of cancer and may induce DNA damage [42]. Mitochondria play crucial roles in the energy metabolism and oxidative stress of glioma [43]. Research on mitochondria-mediated cancer therapy has been conducted [44,45]. Nuclear MTRGs are highly associated with the progression and prognosis of many cancers including breast cancer and bladder cancer [46,47]. However, the potential function of nuclear MTRGs in glioma is still unknown. In this study, we aimed to investigate the association between nuclear MTRGs and the characteristics of glioma.

First, we identified DEGs of glioma and took the intersection of the DEGs and nuclear MTRGs. Subsequently, we utilized LASSO regression and selected 16 prognosis-related genes. The patients were stratified into two distinct clusters by consensus clustering analysis. Cluster One was characterized by features such as high nuclear MTRG expression, low survival rate, increased expression of ICRGs, high TIDE score, and high immune infiltration. Compared to those in Cluster One, Cluster Two had low nuclear MTRG expression, a better survival rate, decreased expression of ICRGs, a low TIDE score, and low immune infiltration. Interestingly, we found that the higher immune signature in Cluster One leads to worse survival. Previous research has reported a negative correlation between glioma-associated macrophages and myeloid dendritic cells with respect to survival [48]. This may be associated with the localization of macrophages in glioma. Scientists have found that tumor-educated macrophages entrenched in the glioma microenvironment play supportive roles in promoting angiogenesis [49]. In addition, in mice, gliomas that developed under CD8⁺ T cell pressure exhibited more malignant histological characteristics compared to gliomas developed without CD8⁺ T cells, which indicates a potential mechanism of immune evasion [50].

The above findings revealed that nuclear MTRGs played complex roles in glioma; therefore, we explored the mutation landscape of the two clusters. Previous research found that tumors with IDH1 or IDH2 mutations had unique clinical and genetic characteristics, and patients with these mutations tended to have better survival [38]. Our findings corroborated those of prior studies. We found that patients in Cluster Two had higher IDH1 or IDH2 mutation rates. Cluster One had a higher frequency of EGFR mutations, which can promote invasion, proliferation, and resistance to chemotherapy [39]. We calculated the IC50 between the two clusters, and Temozolomide, Carmustine, and Dabrafenib had a better effect on Cluster Two. Trametinib had better effect on Cluster One. These findings may contribute to precision medicine for glioma treatment.

Considering the poor survival of gliomas, the construction of an accurate and reliable prognostic model for gliomas appeared to be particularly important. Existing models seldom use machine learning algorithm and had limited verification sets [51,52]. We constructed prognostic models based on multiple machine learning algorithms and previous selected 16 previously nuclear MTRGs. The model constructed by LASSO had the highest AUC and was the most effective model. The model was further verified by three datasets, including the TCGA validation set, CGGA, and GSE184941. Compared to the existing model, our LASSO model is more accurate and reliable, with a better AUC for predicting the prognosis of glioma patients [53–55].

Among the 16 selected nuclear MTRGs, *MGME1* was selected for its vital prognostic ability. *MGME1* is a mitochondria-specific DNase with high conservation [56]. It belongs to the PD-(D/E)XK nuclease superfamily and plays an important role in the replication and degradation of mtDNA. In vitro studies have demonstrated that it possesses the ability to cleave single-stranded DNAs in both the 5'→3' and 3'→5' directions [57]. Moreover, deleterious mutations in *MGME1* may result in significant mitochondrial disorders affecting multiple bodily systems [58]. A previous study revealed that *MGME1* was a possible cancer-promoting molecule in colorectal cancer [59]. Additionally, *MGME1* was found to be associated with poor prognosis of glioma and closely related to the cell proliferation in LGG [60]. However, research on the function of *MGME1* in tumorigenesis is still limited and the function and expression of *MGME1* in the tumor microenvironment, TMB, and MSI are unknown. In our research, we illustrated that *MGME1* was a potential biomarker associated with infiltrating immune cells, ICB therapy, TMB, and MSI in glioma, and *MGME1* also played an important role in the tumor microenvironment, TMB, and MSI across human tumors. Overall, our findings indicated that *MGME1* is not only an effective prognostic biomarker in glioma, but also a potential target in multiple types of tumors.

Despite the valuable insights gained through our study, it is important to acknowledge certain limitations. Specifically, further research utilizing a larger sample size is necessary to enhance the analysis. In addition, we will conduct in vitro and in vivo experimental validation to further confirm our results in the future.

In conclusion, we systematically investigated how nuclear MTRGs contribute to glioma classification and prognosis. Two independent subtypes of glioma based on nuclear MTRGs were identified. These two clusters exhibited divergent prognosis, tumor microenvironment, mutation types of genes, response to ICB therapy, and drug sensitivity. Additionally, we developed a reliable and robust prognostic signature using machine learning algorithms. Furthermore, we highlighted *MGME1* as a novel molecular biomarker in multiple tumors. These results provide potential targets and improve precision medicine for glioma treatment.

Funding

This work was funded by the Doctoral Start-up Foundation of Anhui Medical University (No.0801055201) the National College Students' Innovation and Entrepreneurship Training Program (No. 202210366002), and the College Students' Innovation and Entrepreneurship Training Program of Anhui Province (No. S202210366021 and S202210366017).

Ethics approval statement

Not applicable.

Author contribution statement

Chang Liu; Ning Zhang; Zhihao Xu: Conceived and designed the experiments; Performed the experiments; Analyzed and interpreted the data; Contributed reagents, materials, analysis tools or data; Wrote the paper. Xiaofeng Wang; Yang Yang; Junming Bu; Huake Cao: Performed the experiments; Analyzed and interpreted the data. Jin Xiao: Conceived and designed the experiments; Performed the experiments; Analyzed and interpreted the data; Contributed reagents, materials, analysis tools or data; Wrote the paper. Yinyin Xie: Performed the experiments; Analyzed and interpreted the data; Contributed reagents, materials, analysis tools or data; Wrote the paper.

Data availability statement

Data included in article/supplementary material/referenced in article.

Declaration of competing interest

The authors declare that they have no known competing financial interests or personal relationships that could have appeared to influence the work reported in this paper.

Acknowledgments

We thank the Mathematical Medicine Integration Innovation Training Program for Undergraduate Students (MITUS) for providing valuable guidance, support, research opportunities, and resources.

Appendix A. Supplementary data

Supplementary data to this article can be found online at <https://doi.org/10.1016/j.heliyon.2023.e19856>.

References

- [1] K. Vigneswaran, S. Neill, C.G. Hadjipanayis, Beyond the World Health Organization grading of infiltrating gliomas: advances in the molecular genetics of glioma classification, *Ann. Transl. Med.* 3 (7) (2015) 95.
- [2] M.E. Davis, Epidemiology and overview of gliomas, *Semin. Oncol. Nurs.* 34 (5) (2018) 420–429.
- [3] A. Finch, et al., Advances in research of adult gliomas, *Int. J. Mol. Sci.* 22 (2) (2021).
- [4] Q.T. Ostrom, et al., CBTRUS Statistical Report: primary brain and other central nervous system tumors diagnosed in the United States in 2010–2014, *Neuro Oncol.* 19 (2017) v1–v88 (suppl. 5).
- [5] S. Lapointe, A. Perry, N.A. Butowski, Primary brain tumours in adults, *Lancet (London, England)* 392 (10145) (2018) 432–446.
- [6] D. Bhanja, et al., Association of low-grade glioma diagnosis and management approach with mental health disorders: a MarketScan analysis 2005–2014, *Cancers* 14 (6) (2022).
- [7] R.K. Oberoi, et al., Strategies to improve delivery of anticancer drugs across the blood-brain barrier to treat glioblastoma, *Neuro Oncol.* 18 (1) (2016) 27–36.
- [8] T.A. Bale, M.K. Rosenblum, The 2021 WHO Classification of Tumors of the Central Nervous System: an update on pediatric low-grade gliomas and glioneuronal tumors, *Brain Pathol.* 32 (4) (2022), e13060.
- [9] C. Horbinski, et al., Clinical implications of the 2021 edition of the WHO classification of central nervous system tumours, *Nat. Rev. Neurol.* 18 (9) (2022) 515–529.
- [10] A.M. Molinaro, et al., Genetic and molecular epidemiology of adult diffuse glioma, *Nat. Rev. Neurol.* 15 (7) (2019) 405–417.
- [11] G. Tachon, et al., Prognostic significance of MEOX2 in gliomas, *Mod. Pathol.* 32 (6) (2019) 774–786.
- [12] H. Zhang, et al., PDIA5 is correlated with immune infiltration and predicts poor prognosis in gliomas, *Front. Immunol.* 12 (2021), 628966.
- [13] D.-Y. Hueng, et al., DDX3X biomarker correlates with poor survival in human gliomas, *Int. J. Mol. Sci.* 16 (7) (2015) 15578–15591.
- [14] J. Nunnari, A. Suomalainen, Mitochondria: in sickness and in health, *Cell* 148 (6) (2012) 1145–1159.
- [15] S. Vyas, E. Zaganjor, M.C. Haigis, Mitochondria and cancer, *Cell* 166 (3) (2016) 555–566.
- [16] H. Li, J. Slone, T. Huang, The role of mitochondrial-related nuclear genes in age-related common disease, *Mitochondrion* 53 (2020) 38–47.
- [17] B. Gonzalez, et al., High-throughput sequencing analysis of nuclear-encoded mitochondrial genes reveals a genetic signature of human longevity, *GeroScience* 45 (1) (2023) 311–330.
- [18] Q. Huang, et al., Increased mitochondrial fission promotes autophagy and hepatocellular carcinoma cell survival through the ROS-modulated coordinated regulation of the NFKB and TP53 pathways, *Autophagy* 12 (6) (2016).
- [19] S. Li, et al., FUNDC2 promotes liver tumorigenesis by inhibiting MFN1-mediated mitochondrial fusion, *Nat. Commun.* 13 (1) (2022) 3486.
- [20] S. Frank, et al., The role of dynamin-related protein 1, a mediator of mitochondrial fission, in apoptosis, *Dev. Cell* 1 (4) (2001) 515–525.
- [21] D.C. Chan, Mitochondrial dynamics and its involvement in disease, *Annu. Rev. Pathol.* 15 (2020) 235–259.
- [22] H. Huang, et al., Suppression of mitochondrial ROS by prohibitin drives glioblastoma progression and therapeutic resistance, *Nat. Commun.* 12 (1) (2021) 3720.
- [23] S. Wei, et al., Antitumor activity of a mitochondrial-targeted HSP90 inhibitor in gliomas, *Clin. Cancer Res.: Off. J. Am. Assoc. Cancer Res.* 28 (10) (2022) 2180–2195.
- [24] W. Shen, et al., Sangerbox: a comprehensive, interaction-friendly clinical bioinformatics analysis platform, *iMeta* 1 (3) (2022).
- [25] M.E. Ritchie, et al., Limma powers differential expression analyses for RNA-sequencing and microarray studies, *Nucleic Acids Res.* 43 (7) (2015) e47.

- [26] E.K. Gustavsson, et al., ggtranscript: an R package for the visualization and interpretation of transcript isoforms using ggplot2, *Bioinformatics* 38 (15) (2022) 3844–3846.
- [27] Z. Tang, et al., GEPIA2: an enhanced web server for large-scale expression profiling and interactive analysis, *Nucleic Acids Res.* 47 (W1) (2019) W556–W560.
- [28] G. Yu, et al., clusterProfiler: an R package for comparing biological themes among gene clusters, *OMICS A J. Integr. Biol.* 16 (5) (2012) 284–287.
- [29] G. Sturm, et al., Comprehensive evaluation of transcriptome-based cell-type quantification methods for immuno-oncology, *Bioinformatics* 35 (14) (2019) i436–i445.
- [30] A. Mayakonda, et al., Maftools: efficient and comprehensive analysis of somatic variants in cancer, *Genome Res.* 28 (11) (2018) 1747–1756.
- [31] D. Maeser, R.F. Gruener, R.S. Huang, oncoPredict: an R package for predicting in vivo or cancer patient drug response and biomarkers from cell line screening data, *Briefings Bioinf.* 22 (6) (2021).
- [32] S. Pölsterl, Scikit-survival: a library for time-to-event analysis built on top of scikit-learn, *J. Mach. Learn. Res.* 21 (1) (2020) 8747–8752.
- [33] J.L. Katzman, et al., DeepSurv: personalized treatment recommender system using a Cox proportional hazards deep neural network, *BMC Med. Res. Methodol.* 18 (1) (2018) 1–12.
- [34] K. Kang, et al., Comprehensive exploration of tumor mutational burden and immune infiltration in diffuse glioma, *Int. Immunopharm.* 96 (2021), 107610.
- [35] Y. Eso, et al., Microsatellite instability and immune checkpoint inhibitors: toward precision medicine against gastrointestinal and hepatobiliary cancers, *J. Gastroenterol.* 55 (1) (2020) 15–26.
- [36] L.B. Nabors, et al., Central nervous system cancers, version 3.2020, NCCN clinical practice guidelines in oncology, *J. Natl. Compr. Cancer Netw. : J. Natl. Compr. Cancer Netw.* 18 (11) (2020) 1537–1570.
- [37] P.Y. Wen, et al., Dabrafenib plus trametinib in patients with BRAFV600E-mutant low-grade and high-grade glioma (ROAR): a multicentre, open-label, single-arm, phase 2, basket trial, *Lancet Oncol.* 23 (1) (2022) 53–64.
- [38] H. Yan, et al., IDH1 and IDH2 mutations in gliomas, *N. Engl. J. Med.* 360 (8) (2009) 765–773.
- [39] O. Alexandru, et al., The influence of EGFR inactivation on the radiation response in high grade glioma, *Int. J. Mol. Sci.* 19 (1) (2018).
- [40] F. Mao, et al., LRIG proteins in glioma: functional roles, molecular mechanisms, and potential clinical implications, *J. Neurol. Sci.* 383 (2017) 56–60.
- [41] P.Y. Wen, S. Kesari, Malignant gliomas in adults, *N. Engl. J. Med.* 359 (5) (2008) 492–507.
- [42] X. Renaudin, Reactive oxygen species and DNA damage response in cancer, *Int. Rev. Cell Mol. Biol.* 364 (2021) 139–161.
- [43] C.J.F. van Noorden, et al., Energy metabolism in IDH1 wild-type and IDH1-mutated glioblastoma stem cells: a novel target for therapy? *Cells* 10 (3) (2021).
- [44] G.J. Pilkington, K. Parker, S.A. Murray, Approaches to mitochondrially mediated cancer therapy, *Semin. Cancer Biol.* 18 (3) (2008) 226–235.
- [45] Z. Wu, W.S. Ho, R. Lu, Targeting mitochondrial oxidative Phosphorylation in glioblastoma therapy, *NeuroMolecular Med.* 24 (1) (2022) 18–22.
- [46] L.-R. Yan, et al., Mitochondria-related core genes and TF-miRNA-hub mrDEGs network in breast cancer, *Biosci. Rep.* 41 (1) (2021).
- [47] X. Jiang, et al., Identification of a nuclear mitochondrial-related multi-genes signature to predict the prognosis of bladder cancer, *Front. Oncol.* 11 (2021), 746029.
- [48] A. Gieryng, et al., Immune microenvironment of gliomas, *Lab. Invest.: a J. Tech. Methods Pathol.* 97 (5) (2017) 498–518.
- [49] D.P. Radin, S.E. Tsirka, Interactions between tumor cells, neurons, and microglia in the glioma microenvironment, *Int. J. Mol. Sci.* 21 (22) (2020).
- [50] J.R. Kane, et al., CD8+ T-cell-mediated immunoeediting influences genomic evolution and immune evasion in Murine gliomas, *Clin. Cancer Res.: Off. J. Am. Assoc. Cancer Res.* 26 (16) (2020) 4390–4401.
- [51] H. Zhang, et al., Identification of a fibroblast-related prognostic model in glioma based on bioinformatics methods, *Biomolecules* 12 (11) (2022).
- [52] F. Wu, et al., Prognostic power of a lipid metabolism gene panel for diffuse gliomas, *J. Cell Mol. Med.* 23 (11) (2019) 7741–7748.
- [53] X. Liang, et al., Promoting prognostic model application: a review based on gliomas, *J. Oncol.* 2021 (2021), 7840007.
- [54] X. Bingxiang, et al., A prognostic model for brain glioma patients based on 9 signature glycolytic genes, *BioMed Res. Int.* 2021 (2021), 6680066.
- [55] P. Del Bianco, et al., Myeloid diagnostic and prognostic markers of immune suppression in the blood of glioma patients, *Front. Immunol.* 12 (2021), 809826.
- [56] R.J. Szczesny, et al., Identification of a novel human mitochondrial endo-/exonuclease Ddk1/c20orf72 necessary for maintenance of proper 7S DNA levels, *Nucleic Acids Res.* 41 (5) (2013) 3144–3161.
- [57] T.J. Nicholls, et al., Linear mtDNA fragments and unusual mtDNA rearrangements associated with pathological deficiency of MGME1 exonuclease, *Hum. Mol. Genet.* 23 (23) (2014) 6147–6162.
- [58] C. Kornblum, et al., Loss-of-function mutations in MGME1 impair mtDNA replication and cause multisystemic mitochondrial disease, *Nat. Genet.* 45 (2) (2013) 214–219.
- [59] Q. Wang, et al., Age-stratified proteomic characteristics and identification of promising precise clinical treatment targets of colorectal cancer, *J. Proteomics* 277 (2023), 104863.
- [60] F. Xiao, et al., MGME1 associates with poor prognosis and is vital for cell proliferation in lower-grade glioma, *Aging* 15 (9) (2023) 3690–3714, declarations.